Old Dogs and Their Ancient Tricks: How Cutting-Edge Structural Methods Gave Us New Insight into Ancient Molecules

Cutting-edge techniques revealed for the first time the undistorted atomic structure of ancient molecules when interacting with proteins in different redox states. These pristine structures permit a more detailed understanding of how proteins modulate energy conversion in biology.

From sensing their environments to metabolism, all living beings rely on proteins for their biological activities. However, for some special functions such as respiration, the electron transfer reaction by which animals transform food and oxygen into energy and waste products, proteins are insufficient. In these crucial cases, specialized molecules called cofactors are combined with proteins to expand the latter's functionality. Iron-sulfur clusters[1] (FeS, **Fig. 1(a)**) and flavins[2] (**Fig. 1(b)**) are two of the most ancient cofactors used during electron transfer. While FeS are small, inorganic compounds that accept or release a single electron (**Fig. 1(a)**), flavins, and more specifically flavin adenine dinucleotide (FAD), are larger organic molecules (**Fig. 1(b)**) with complex electron chemistry. In fact, FAD can either accept or donate up to two electrons, resulting in three possible redox states (**Fig. 1(b)**): fully depleted (FAD_{ox}), harboring one electron ($FAD^{\bullet-}$), or two ($FADH^-$).[3] Because of its redox versatility, proteins commonly use FAD as an adaptor between two-electron donors/acceptors, such as food-derived sugars and oxygen, and single-electron cofactors, such as FeS. Here, it has been suggested that proteins can modulate FAD and FeS redox properties *via* subtly changing their structures.

Given their enormous biochemical importance and intriguing structure-function relationship, FAD- and FeS-containing proteins have been extensively studied using structural methods such as X-ray crystallography and cryo-electron microscopy. However, both techniques release electrons during data collection, which are then captured by FAD and FeS cofactors.[4,5] Even a few milliseconds of data collection may alter the cofactor's redox state and cause structural distortions. This limitation in capturing native-like structures has left the natural mechanisms by which proteins interact with their cofactors under defined redox conditions unclear.

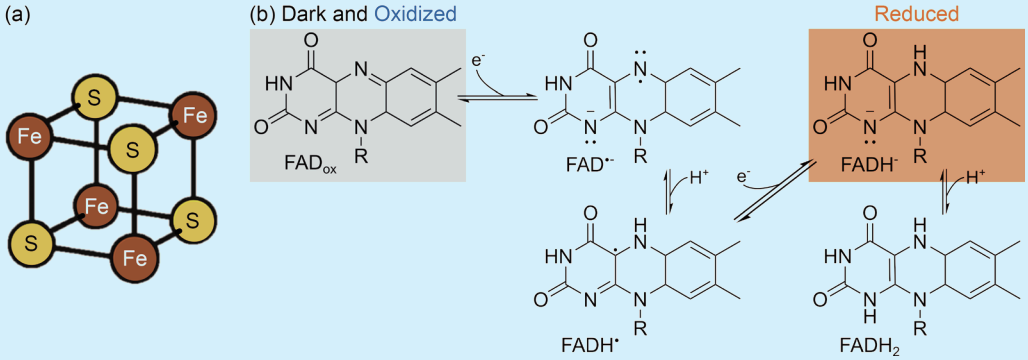

Fig. 1: The co-factors of *Cc*(6-4)PL. (a) The iron sulfur cluster FeS. An iron sulfur cluster consists of four sulfur and four iron atoms (yellow and orange, respectively), which arrange themselves in a cubic shape. The iron atoms then interact with the protein *via* sulfur-containing amino acids called cysteines. (b) The redox chemistry of FAD. Oxidized FAD (FAD_{ox}) transforms into $FAD^{\bullet-}$ by capturing an electron. $FAD^{\bullet-}$ can then evolve into $FADH^\bullet$ *via* addition of a proton (H^+). A second electron capture produces $FADH^-$ from $FADH^\bullet$. A final proton capture may produce $FADH_2$. In the dark-adapted and oxidized states, *Cc*(6-4)PL contains FAD_{ox} (grey shade), while in its reduced form, it contains $FADH^-$ (orange shade).

Here, an international research team led by Maestre-Reyna (National Taiwan University and Academia Sinica) and Essen (Philipps University Marburg, Germany) determined, for the first time, the structures of undistorted FeS and FAD working in tandem within a single protein, and in several different redox states (**Fig. 2**, see next page).[6] To do so, the international team used damage-free serial femtosecond crystallography (DF-SFX), a cutting-edge technique that can only be conducted in X-ray free electron lasers, special X-ray sources of which there are only five in the world. Because DF-SFX data collection is much faster than redox chemistry, the cofactors in structures obtained *via* DF-SFX maintain their native, redox-defined states.[7] For comparison purposes, the researchers also used the **TPS 05A** to produce radiation-damaged structures.

The chosen model system was the *Caulobacter crescentus* 64 photolyase (*Cc*(6-4)PL), an FAD-containing protein capable of using the energy of blue light to inject electrons into its flavin cofactor. Once the FAD is fully reduced ($FADH^-$), *Cc*(6-4)PL can then use the cofactor to repair mutated DNA. Interestingly, *Cc*(6-4)PL also contained a single FeS, whose function is not well understood.[8,9] To determine the *Cc*(6-4)PL undistorted structures of both the FAD and FeS in different redox states, and to determine whether the FeS redox chemistry depended on that of FAD, Prof. Maestre-Reyna's team collected the structure of *Cc*(6-4)PL in three different states. First, by performing the DF-SFX experiment in the dark, they collected dark-adapted *Cc*(6-4)PL (FAD_{ox}-FeS^{2+} state, **Fig. 2(a)**). By applying strong blue light and an electron donor, they induced full reduction of the FAD *via* illumination ($FADH^-$-FeS^{2+} state, **Fig. 2(a)**). Finally, by exposing the protein to an FeS-specific oxidizing agent, they obtained the oxidized *Cc*(6-4)PL structure (FAD_{ox}-FeS^{3+} state, **Fig. 2(a)**).

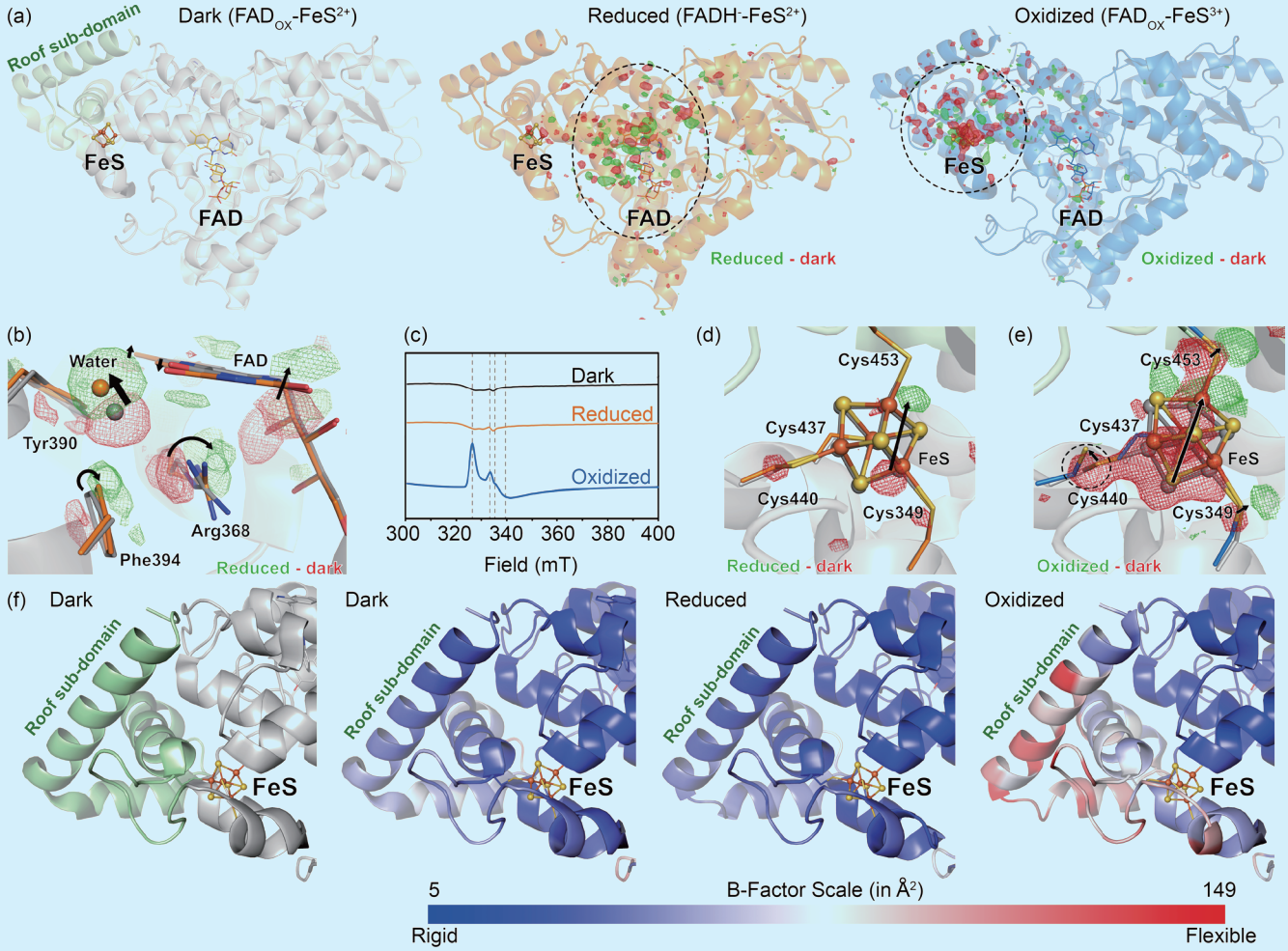

Fig. 2: The undistorted structures of *Cc*(6-4)PL in different redox states. (a) Global structures of *Cc*(6-4)PL in different redox states. Left: Dark-adapted state (grey cartoon with roof sub-domain shown in green), middle: reduced state (orange cartoon), right: oxidized state (blue cartoon). Difference electron density maps comparing the corresponding structure vs. the dark state are shown over the reduced and oxidized structures (green for positive peaks, red for negative ones). Difference electron density highlights where changes are occurring in the structure upon change of state, with negative features indicating locations from which atoms depart, while positive features where they move towards. The region of change is further highlighted with a black dashed circle. (b) Detail of the reduced vs. dark structural changes around the FAD binding site. Arrows indicate the direction of motion of individual amino acids (from negative towards positive density). Amino acids are shown as sticks (grey for dark, orange for reduced). (c) Electron paramagnetic resonance spectra of *Cc*(6-4)PL in the three redox states studied in this work (black for dark, orange for reduced, blue for oxidized). Notice that the dark and reduced states show the same spectrum, indicating no FeS redox change. The different shape of the spectrum in the oxidized state is indicative of oxidation of FeS. (d) Detail of the reduced vs. dark structural changes around the FeS binding site. Arrows indicate the direction of motion of individual amino acids (from negative towards positive density). Amino acids are shown as sticks, while FeS atoms as spheres (grey for dark, orange for reduced). (e) Detail of the oxidized vs. dark structural changes around the FeS binding site. Arrows indicate the direction of motion of individual amino acids (from negative towards positive density). Amino acids are shown as sticks, while FeS atoms as spheres (grey for dark, blue for oxidized). The broken protein–FeS bond is highlighted with a dashed black circle. (f) FeS redox state-dependent changes in the roof sub-domain. Left: Detail of the dark-adapted roof sub-domain shown as in (a). Right: Roof sub-domain in each of the *Cc*(6-4)PL, as indicated over each panel. Structures are shown as cartoons, and are colored by B-factor (blue to red), which is a measurement of protein flexibility. A color scale is provided below the panels. While the roof sub-domain is very rigid (blue) in the dark and reduced states, it is very flexible (red) in the oxidized state. [Adapted from Ref. 6]

By comparing the dark-adapted vs. reduced FAD states, the researchers found that the FAD underwent a "butterfly bend" along its three-membered ring moiety (**Fig. 2(b)**). Importantly, this redox state change induced dramatic changes in the *Cc*(6-4)PL protein, which compensated for the extra negative charge on $FADH^-$ by positioning a positively charged residue, Arginine R368, close to $FADH^-$ (**Fig. 2(b)**). Furthermore, a nearby water molecule moved away from the FAD upon reduction, suggesting that it acted as a proton donor during FAD reduction (**Figs. 2(b) and 1(b)**). Nearby aromatic residues also changed their conformation (**Fig. 2(b)**), supporting their role in electron transfer toward the FAD. Although independent electron paramagnetic resonance experiments (**Fig. 2(c)**) showed that FeS did not change its redox state in response to FAD transitioning to $FADH^-$, the team's research highlighted the tight correlation between FAD and FeS, as *Cc*(6-4)PL adaptation to $FADH^-$ resulted in subtle changes in FeS 3D structure (**Fig. 2(d)**). Conversely, *Cc*(6-4)PL responded to oxidation of FeS by partially breaking a single iron–protein bond (**Fig. 2(e)**). As a result, a *Cc*(6-4)PL region crucial for DNA recognition, the roof-like domain, became highly flexible (**Fig. 2(f)**), potentially impairing DNA binding. This revealed the structural basis by which FeS-containing DNA-binding proteins couple their ability to recognize DNA to the FeS redox state.

Overall, the joint research by the Maestre-Reyna and Essen groups revealed the structure–function relationship of a set of ancient cofactors by using the cutting-edge methodologies such as DF-SFX, showing for the first time how these old dogs perform their ancient tricks. Furthermore, their research has opened the path towards understanding the dynamics of FAD and FeS interlinked redox chemistry *via* time-resolved crystallographic methods. (Reported by Manuel Maestre-Reyna, National Taiwan University and Academia Sinica)

This report features the work of Manuel Maestre-Reyna and his collaborators published in J. Am. Chem. Soc. ***147****, 16084 (2025).*

TPS 05A Protein Microcrystallography

- Protein Crystallography
- Biological Macromolecules, Protein Structures, Life Science

References

1. R. Lill, Nature **460**, 831 (2009).
2. R. L. Fagan, B. A. Palfey. Elsevier Ltd, 37 (2010).
3. M. Maestre-Reyna, C. H. Yang, E. Nango, W. C. Huang, E. P. G. Ngurah Putu, W. J. Wu, P. H. Wang, S. Franz-Badur, M. Saft, H. J. Emmerich, H. Y. Wu, C. C. Lee, K. F. Huang, Y. K. Chang, J. H. Liao, J. H. Weng, W. Gad, C. W. Chang, A. H. Pang, M. Sugahara, S. Owada, Y. Hosokawa, Y. Joti, A. Yamashita, R. Tanaka, T. Tanaka, F. Luo, K. Tono, K. C. Hsu, S. Kiontke, I. Schapiro, R. Spadaccini, A. Royant, J. Yamamoto, S. Iwata, L. O. Essen, Y. Bessho, M. D. Tsai, Nat. Chem. **14**, 677 (2022).
4. E. F. Garman, Acta Crystallogr. D Biol. Crystallogr. **66**, 339 (2010).
5. V. Pfanzagl, J. H. Beale, H. Michlits, D. Schmidt, T. Gabler, C. Obinger, K. Djinović-Carugo, S. Hofbauer, J. Biol. Chem. **295**, 13488 (2020).
6. P. H. Wang, Y. Hosokawa, J. C Soares, H. J. Emmerich, V. Fuchs, N. Caramello, S. Engilberge, A. Bologna, C. J. Rosner, M. Nakamura, M. Watad, F. Luo, S. Owada, T. Tosha, J. Kang, K. Tono, Y. Bessho, E. Nango, A. J. Pierik, A. Royant, M. D. Tsai, J. Yamamoto, M. Maestre-Reyna, L. O. Essen, J. Am. Chem. Soc. **147**, 16084 (2025).
7. H. N. Chapman, C. Caleman, N. Timneanu, Phil. Trans. R. Soc. B **369**, 20130313 (2014).
8. K. Hitomi, K. Okamoto, H. Daiyasu, H. Miyashita, S. Iwai, H. Toh, M. Ishiura, T. Todo, Nucleic Acids Res. **28**, 2353 (2000).
9. I. Oberpichler, A. J. Pierik, J. Wesslowski, R. Pokorny, R. Rosen, M. Vugman, F. Zhang, O. Neubauer, E. Z. Ron, A. Batschauer, T. Lamparter, PLoS One **6**, e26775 (2011).